IEEE Access
Multidisciplinary | Rapid Review | Open Access Journal

Received November 21, 2019, accepted December 23, 2019, date of publication January 13, 2020, date of current version January 24, 2020.

Digital Object Identifier 10.1109/ACCESS.2020.2966262

Novel Diplexer and Triplexer Designs Avoiding Additional Matching Circuits Outside Filters

PU-HUA DENG[1], (Member, IEEE), SHENG-WEI LEI[2], WEI LO[3], AND MING-WEI LI[4]
[1]Department of Electrical Engineering, National University of Kaohsiung, Kaohsiung 811, Taiwan
[2]MediaTek, Hsinchu 30078, Taiwan
[3]Super Micro Computer, San Jose, CA 95131, USA
[4]Institute of Photonics Technologies, National Tsing Hua University, Hsinchu 30071, Taiwan

Corresponding author: Pu-Hua Deng (phdeng@nuk.edu.tw)

This work was supported by the Ministry of Science and Technology, Taiwan, under Grant MOST 105-2221-E-390-003, Grant MOST 106-2221-E-390-009, and Grant MOST 107-2221-E-390-007.

ABSTRACT Diplexers and triplexers are widely used in communication systems for separating frequency bands in different channels. Design issues related to preventing additional matching circuits, integrating two or three band input resonators into one-band resonator size, systematically designing each band external quality factor (Q_L), and avoiding loading effects are often encountered. To overcome these bottlenecks, stub-loaded resonators that feature in various negligible band loading effects are used to design proposed diplexers and triplexers. In particular, the stub-loaded resonator (SLR), used in the proposed triplexers and costing only one-band resonator size, achieves a negligible loading effect systematic procedure for designing the three bands required as external quality factors and resonant frequencies. Each SLR of the triplexers uses an integrated matching circuit in the resonator instead of an additional matching circuit outside the resonator. To our knowledge, a tapped-line feed resonator that can independently design three band external quality factors (Q_{Ls}) and meet matching requirements by using one-band resonator size has not been reported thus far. All the currently proposed circuits have been verified and fabricated on RO4003C substrates.

INDEX TERMS Diplexer, external quality factor, loading effect, matching, quarter wavelength, resonator, stub-loaded, triplexer.

I. INTRODUCTION

Diplexers [1]–[15] and triplexers or multiplexers [3], [5], [16]–[30] are used for splitting multifrequency band signals to different channels. In [1]–[14], the diplexers are bandpass responses for their transmission channels. To separate intermediate frequency and local oscillator signals, [15] proposed lowpass-bandpass diplexer. Moreover, [1] and [4]–[11] have proposed compact diplexers; [2]–[7], [12], and [14] have proposed them for high selectivity and effective isolation. However, a matching circuit may be a difficult design when the channel number of a multiplexer is >2. For instance, each channel matching line of the triplexer [28] requires meeting two frequency open conditions simultaneously, which may be time-consuming process. Although studies such as [16], [20], [27], and [31] have proposed systematic matching designs, the matching circuits are needed outside the filters and typically cost additional lumped elements or large transmission line circuit sizes. Diplexer, triplexers, and multiplexers can avoid additional matching circuits outside the filters [9], [13], [18], [19], [21], [24]. However, they likely resolve the problem of external quality factor (Q_L) realization because the distance between resonator and distributed-feed line is typically restricted by process limitations, particularly for high dielectric constants and thin substrates. Moreover, the length of the distributed-feed line is generally long when the number of circuit channels is high and results in a large size; each input resonator must be carefully selected with coupled locations with distributed-feed lines because they are unsuitable for designing the required Q_L universally (e.g., [18]). In general, a diplexer, triplexer, or multiplexer using distributed-feed line structure is suitable for realizing narrowband filter responses because the distance between each resonator and feeding line is restricted.

In diplexers and triplexers or multiplexers, matching circuits can provide independently simple design for each

The associate editor coordinating the review of this manuscript and approving it for publication was Xiu Yin Zhang.

channel filter response. In general, a matching circuit is not difficult in non-wideband diplexer design because each channel only needs one open narrowband condition to be easily met using two additional matching lines outside the filters (e.g., [1]–[3], [5], [7], [12]). To avoid using additional matching circuits outside the filters, common resonators have been proposed [6] and [8]. However, each band Q_L cannot be designed independently, resulting in increasing difficulty for designing each band response. For instance, in [6] two-band Q_{Ls} are determined simultaneously when one tap point of the common resonator is selected. [14] successfully proposed diplexers without extra matching circuits and two band responses could be independently designed. However, there were no shared circuits for two band filters which might affect the circuit integrations.

A branch-line resonator (BLR) with independent design for two-band external quality factors was first proposed for dual-band filters in [32], and then a similar structure was reported in [33], with one segment of the transmission line removed from the resonator structure in [32]. The BLR of in [32] or [33] can also be used as the first shared resonator of a diplexer that can independently design each band Q_L without additional matching circuits outside the filters. In [32] or [33], the BLR needed two λ/4 transmission lines in the matching circuits, but occasionally, integrating two λ/4 transmission lines into the BLR may be difficult. To resolve this problem, this study used only one λ/4 matching line integrated in a resonator to form the proposed stub-loaded resonator SLR D. An independent design for dual-band Q_{Ls} was achieved. By using the proposed SLR D, two diplexers were proposed. Compared with the diplexer [12] that used stub-loaded resonators, each of the proposed diplexers did not require matching lines outside the filters without loading effects for each operating band circuit. The first two-band resonators in each presented diplexer integrated to form one stub-loaded resonator, i.e., each of the proposed diplexers saved one resonator near the input port.

By integrating two λ/4 matching lines in a resonator, a stub-loaded resonator SLR T was proposed as a systematic design for two triplexers without loading effects. Compared with the triplexers [16], the proposed triplexers without additional matching circuits outside the filters can have independent Q_L designs for each filter. Furthermore, the proposed SLR T integrates three band resonators into one-band resonator size. Although the triplexer of [8] did not require matching circuits outside the filters and used common resonators to achieve compact purpose, no independent design for each band Q_L near the input port resonator, which provides a simple design for each band response, can be obtained.

II. DISCUSSION OF CONVENTIONAL AND PROPOSED DIPLEXERS

Fig. 1(a) illustrates a conventional diplexer by using two tapped-line feed third-order filters [35]. Two matching lines $\mathbf{X_{M1}^{(D)}}$ and $\mathbf{X_{M2}^{(D)}}$ are added outside two-band third-order filters BPF A^D and BPF B^D to prevent a loading effect.

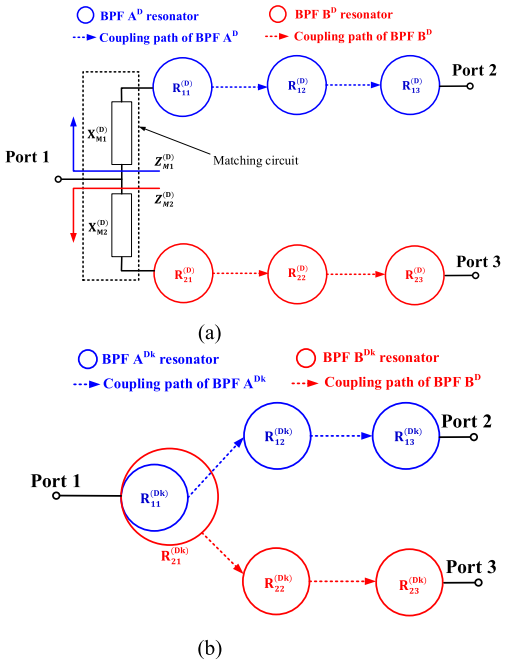

FIGURE 1. Using tapped-line feed third-order filters for (a) conventional and (b) proposed diplexers.

The proposed diplexer illustrated in Fig. 1(b) includes two third-order filters BPF A^{DK} and BPF B^{DK}, the center frequencies of which are f_1 and f_2, respectively. Resonator $\mathbf{R_{11}^{(Dk)}}$ is part of resonator $\mathbf{R_{21}^{(Dk)}}$ at the input port; the external quality factor and resonance frequency of each band resonator can be systematically designed using integrated matching lines. Compared with a conventional diplexer (Fig. 1(a)), the proposed diplexer of Fig. 1(b) uses only one resonator (resonator $\mathbf{R_{21}^{(Dk)}}$)-sized circuit to replace the similar role played by $\mathbf{X_{M1}^{(D)}}$, $\mathbf{X_{M2}^{(D)}}$, resonator $\mathbf{R_{11}^{(D)}}$, and resonator $\mathbf{R_{21}^{(D)}}$.

III. DESIGN OF THE PROPOSED DIPLEXER RESONATOR

The proposed stub-loaded resonator SLR D consists of four transmission lines $X_{T1}^{(D)}$, $X_{T2}^{(D)}$, $X_{T3}^{(D)}$, and $X_{T4}^{(D)}$, with a load impedance $Z_{S/O}^{(D)}$ at the right end of $X_{T4}^{(D)}$, as shown in Fig. 2, wherein $Z_{S/O}^{(D)}$ can be designed as an open or short circuit, making the SLR D similar to the stub-loaded resonator in [12] or the net-type resonator in [34].

The proposed SLR D is operated to resonate at two desired frequencies f_1 and f_2. The first three transmission lines $X_{T1}^{(D)}$, $X_{T2}^{(D)}$, and $X_{T3}^{(D)}$ are enclosed in the blue line form of the first resonator, $R_1^{(D1)}$, which resonates at f_1, and all the transmission lines $X_{T1}^{(D)}$, $X_{T2}^{(D)}$, $X_{T3}^{(D)}$, and $X_{T4}^{(D)}$ with $Z_{S/O}^{(D)}$ are enclosed in the red line form of the other resonator, $R_1^{(D2)}$, which resonates at f_2, wherein $\theta_{Ti}^{(D)}$ and $Z_{Ti}^{(D)} = 1/Y_{Ti}^{(D)}$, $i = 1, 2, 3$, or 4, represent electrical length and characteristic impedance, respectively. Because the length of $X_{T3}^{(D)}$ is designed to be equal to $\lambda/4$ at f_1, Point B_D is a short circuit, causing the admittance $Y_{in2}^{(D)}$ of f_1 to approach no loading

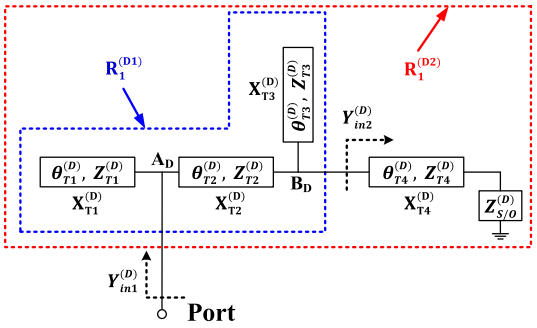

FIGURE 2. Proposed SLR D structure.

effect for $R_1^{(D1)}$. The total lengths of $X_{T1}^{(D)}$, $X_{T2}^{(D)}$, and $X_{T3}^{(D)}$ are $\lambda/2$ of f_1, and the characteristic impedance of $X_{T1}^{(D)}$ equals that of $X_{T2}^{(D)}$(i.e., $R_1^{(D1)}$ composed of $X_{T1}^{(D)}$, $X_{T2}^{(D)}$, and $X_{T3}^{(D)}$ is a $\lambda/2$ resonator at f_1). The Q_L of $R_1^{(D1)}$ can be designed by adjusting the length ratio of $\theta_{T1}^{(D)}$ and $\theta_{T2}^{(D)}$, such as by using the tapped-line feed coupled-resonator filter [35].

The resonant frequency and Q_L of a resonator can be determined by the following equations [36]

$$Y_{in} = 0 \tag{1}$$

$$Q_L = R_L \frac{\omega_0}{2} \frac{dB}{d\omega}|_{\omega=\omega_0} \tag{2}$$

where Y_{in} is the input admittance; $R_L = 50\Omega$ that equals system impedance is the input impedance from resonator to input port load; ω and ω_0 are the angular frequency variable and resonant angular frequency, respectively; and B is the imaginary part of Y_{in}.

Resonant condition of $R_1^{(D2)}$ at f_2 can be obtained by substituting the input admittance $Y_{in1}^{(D)}$ into (1). When the filter response specification at f_2 is determined, the required Q_L of (2) is obtained. Equations (1) and (2) include eight design parameters of $R_1^{(D2)}$, which are $\theta_{Ti}^{(D)}$ and $Z_{Ti}^{(D)}$, $i = 1-4$. $\theta_{Ti}^{(D)}$ and $Z_{Ti}^{(D)}$, $i = 1-3$, are fixed and well-known when the design of resonator $R_1^{(D1)}$ at f_1 is determined. The remaining two parameters $\theta_{T4}^{(D)}$ and $Z_{T4}^{(D)}$ can be solved using (1) and (2). Furthermore, the resonant frequency and external quality factor of $R_1^{(D1)}$ can also be designed using (1) and (2).

Based on the proposed SLR D design, each Q_L of resonators $R_1^{(D1)}$ and $R_1^{(D2)}$ can be systematically and separately designed.

The SLR D with $Z_{S/O}^{(D)} = \infty\Omega$ and $Z_{S/O}^{(D)} = 0\Omega$ can be used for designing the input resonators of Diplexer A and Diplexer B, respectively. The detailed equations of input admittance and external quality factor using (1) and (2) are shown as follows:

$$Y_{in1}^{(D)} = j\left(Y_{T1}^{(D)}\tan\theta_{T1}^{(D)} + Y_{T2}^{(D)}\cot\theta_{T2}^{(D)} \times \frac{Y_{T2}^{(D)}\tan\theta_{T2}^{(D)}\cot\theta_{T3}^{(D)} + Y_{T3}^{(D)} + a_0\cot\theta_{T3}^{(D)}}{Y_{T2}^{(D)}\cot\theta_{T2}^{(D)}\cot\theta_{T3}^{(D)} - Y_{T3}^{(D)} - a_0\cot\theta_{T3}^{(D)}}\right) = 0 \tag{3}$$

$$\begin{aligned} Q_L^{(D)}|_{f=f_2} &= 25[a_1 - \frac{Y_{T2}^{(D)}\cot\theta_{T2}^{(D)}\,(a_2+a_3+a_4)\,(-a_6-a_7+a_8-a_9)}{(-a_2-a_4+a_5)^2} \\ &+ \frac{Y_{T2}^{(D)}\cot\theta_{T2}^{(D)}\,(-a_8+a_9+a_{10}-a_{11})}{(-a_2-a_4+a_5)} \\ &- \frac{\theta_{T2}^{(D)}Y_{T2}^{(D)}\csc^2\theta_{T2}^{(D)}\,(a_2+a_3+a_4)}{(-a_2-a_4+a_5)}] \end{aligned} \tag{4}$$

where

$$a_0 = \begin{cases} Y_{T4}^{(D)}\tan\theta_{T4}^{(D)}, & Z_{S/O}^{(D)} = \infty\Omega \\ -Y_{T4}^{(D)}\cot\theta_{T4}^{(D)}, & Z_{S/O}^{(D)} = 0\Omega \end{cases} \tag{5a}$$

$$a_1 = \theta_{T1}^{(D)}Y_{T1}^{(D)}\sec^2\theta_{T1}^{(D)} \tag{5b}$$

$$a_2 = \begin{cases} Y_{T4}^{(D)}\cot\theta_{T3}^{(D)}\tan\theta_{T4}^{(D)}, & Z_{S/O}^{(D)} = \infty\Omega \\ -Y_{T4}^{(D)}\cot\theta_{T3}^{(D)}\cot\theta_{T4}^{(D)}, & Z_{S/O}^{(D)} = 0\Omega \end{cases} \tag{5c}$$

$$a_3 = Y_{T2}^{(D)}\tan\theta_{T2}^{(D)}\cot\theta_{T3}^{(D)} \tag{5d}$$

$$a_4 = Y_{T3}^{(D)} \tag{5e}$$

$$a_5 = Y_{T2}^{(D)}\cot\theta_{T2}^{(D)}\cot\theta_{T3}^{(D)} \tag{5f}$$

$$a_6 = \theta_{T3}^{(D)}Y_{T2}^{(D)}\cot\theta_{T2}^{(D)}\csc^2\theta_{T3}^{(D)} \tag{5g}$$

$$a_7 = \theta_{T2}^{(D)}Y_{T2}^{(D)}\csc^2\theta_{T2}^{(D)}\cot\theta_{T3}^{(D)} \tag{5h}$$

$$a_8 = \begin{cases} \theta_{T3}^{(D)}Y_{T4}^{(D)}\csc^2\theta_{T3}^{(D)}\tan\theta_{T4}^{(D)}, & Z_{S/O}^{(D)} = \infty\Omega \\ -\theta_{T3}^{(D)}Y_{T4}^{(D)}\csc^2\theta_{T3}^{(D)}\cot\theta_{T4}^{(D)}, & Z_{S/O}^{(D)} = 0\Omega \end{cases} \tag{5i}$$

$$a_9 = \begin{cases} \theta_{T4}^{(D)}Y_{T4}^{(D)}\cot\theta_{T3}^{(D)}\sec^2\theta_{T4}^{(D)}, & Z_{S/O}^{(D)} = \infty\Omega \\ \theta_{T4}^{(D)}Y_{T4}^{(D)}\cot\theta_{T3}^{(D)}\csc^2\theta_{T4}^{(D)}, & Z_{S/O}^{(D)} = 0\Omega \end{cases} \tag{5j}$$

$$a_{10} = \theta_{T2}^{(D)}Y_{T2}^{(D)}\sec^2\theta_{T2}^{(D)}\cot\theta_{T3}^{(D)} \tag{5k}$$

$$a_{11} = \theta_{T3}^{(D)}Y_{T2}^{(D)}\tan\theta_{T2}^{(D)}\csc^2\theta_{T3}^{(D)}. \tag{5l}$$

TABLE 1. Input circuit comparisons between proposed diplexers and previous diplexers/dual-band filters.

	[2]	[3]	[5]	[6]	[8]	[9]	[12]	[14]	[33]	[34]	DA/DB
1*	y	y	y	n	n	n	y	n	n	n	n
2*	y	y	y	n	n	n	y	y	y	y	y
3*	n	n	n	n	n	y	n	n	n	n	n
4*	0	0	0	0	0	0	0	0	2	2	1
5*	n	n	n	y	y	y	n	n	y	y	y

1*: additional matching circuit outside the filters; 2*: independent Q_L designs for two-band input resonators or independent designs for two-band input circuits of filters; 3*: Q_L realization restricted by the distance between distributed-feed line and input resonator or long distributed-feed line length; 4*: number of integrated $\lambda/4$ matching lines in input resonator; 5*: two-band input resonators integrated in one-band input resonator size; DA: Diplexer A; DB: Diplexer B; y: yes; n: no.

Table 1 lists input circuit comparisons between proposed diplexers and previous diplexers/dual-band filters.

IV. DESIGN OF THE PROPOSED DIPLEXER

Fig. 3 demonstrates the proposed diplexer structure, which has a third-order response in each transmission band, and the design procedure described as follows.

Step I[D]: The input resonator can follow the aforementioned SLR D in Section III to design two-band resonance

TABLE 2. Design parameters of Diplexer A (DA) and Diplexer B (DB).

	f_1/f_2 (GHz)	$\theta_{T1}^{(D)}$ at f_1	$\theta_{T2}^{(D)}$ at f_1	$\theta_{T3}^{(D)}$ at f_1	$\theta_{T4}^{(D)}$ at f_1
	$Q_L^{(D1)}/Q_L^{(D2)}$				
	$M_{12}^{(D1)}/M_{12}^{(D2)}$	$Z_{T1}^{(D)}$ (Ω)	$Z_{T2}^{(D)}$ (Ω)	$Z_{T3}^{(D)}$ (Ω)	$Z_{T4}^{(D)}$ (Ω)
	$M_{23}^{(D1)}/M_{23}^{(D2)}$				
DA	2.4/3.6	73.99°	16.01°	90°	37.26°
	17.21/22.13				
	0.059/0.046	60	60	60	44.3
	0.059/0.046				
DB	2.4/2	77.95°	12.05°	90°	11.99°
	23.79/11.06				
	0.043/0.092	57.6	57.6	30	30
	0.043/0.092				

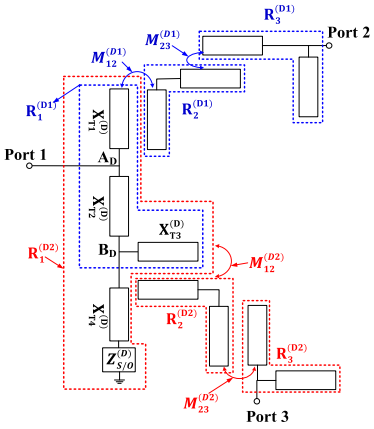

FIGURE 3. Proposed diplexer structure.

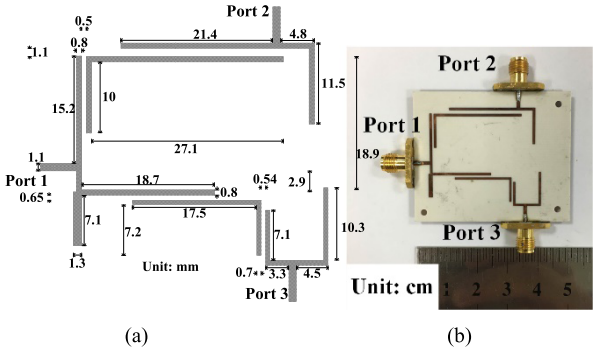

FIGURE 4. (a) Layout and (b) photograph of Diplexer A.

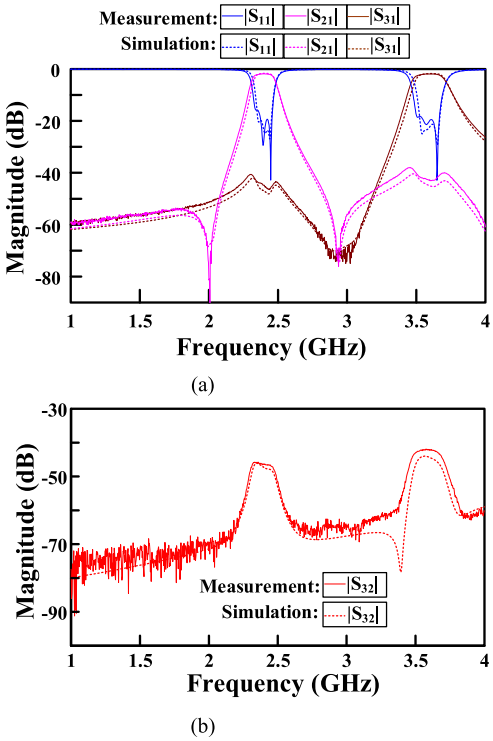

FIGURE 5. Measured and full-wave simulated results of Diplexer A. (a) $|S_{11}|$, $|S_{21}|$, and $|S_{31}|$, and (b) $|S_{32}|$.

frequencies and external quality factors $Q_L^{(D1)}$ (for $R_1^{(D1)}$) and $Q_L^{(D2)}$ (for $R_1^{(D2)}$) based on the desired specification. The matching line $X_{T3}^{(D)}$ is one part of the SLR D and is equal to $\lambda/4$ at f_1. Thus, the loading effect of $X_{T4}^{(D)}$ with $Z_{S/O}^{(D)}$ to $R_1^{(D1)}$ at f_1 can be avoided without adding additional matching circuit.

Step II^D: Each band coupling coefficients are obtained using the tapped-line feed coupled-resonator filter [35] design. In Fig. 3, $M_{ij}^{(D1)}$ represents the coupling coefficient between resonators $R_i^{(D1)}$ and $R_j^{(D1)}$ at f_1; and $M_{ij}^{(D2)}$ represents the coupling coefficient between resonators $R_i^{(D2)}$ and $R_j^{(D2)}$ at f_2. The coupling $M_{12}^{(D1)}$ around f_2 approaches zero because resonators $R_1^{(D1)}$ and $R_2^{(D1)}$ do not approach their resonant frequency f_2. In other words, the loading effect of $R_1^{(D1)}$ from $R_2^{(D1)}$ to the Port 2 load can be ignored around f_2. Similarly, the loading effect of $R_1^{(D2)}$ from $R_2^{(D2)}$ to Port 3 load can be ignored around f_1. Therefore, $R_1^{(D1)}$ and $R_1^{(D2)}$ can design their coupling paths independently; a similar design concept has been validated in [6], [32], and [33].

Step III^D: Output external quality factors of $R_3^{(D1)}$ and $R_3^{(D2)}$ are equal to $Q_L^{(D1)}$ and $Q_L^{(D2)}$, respectively. The Q_{Ls} can be determined by the feeding point, which extraction method is in [35].

Two operating bands of microstrip Diplexer A ($Z_{S/O}^{(D)} = \infty\Omega$) and Diplexer B ($Z_{S/O}^{(D)} = 0\Omega$) are designed with 0.1 dB equal ripple filter responses. The related design parameters are shown in Table 2. Fig. 4 shows the layout and photograph of microstrip Diplexer A, wherein $R_2^{(D1)}$, $R_3^{(D1)}$, $R_2^{(D2)}$, and $R_3^{(D2)}$ use $\lambda/2$ uniform impedance resonators (UIRs). The RO4003C substrate parameters are used for all the proposed circuits. Dielectric constant, loss tangent, and thickness of the substrate are 3.65, 0.065, and 0.508 mm, respectively. Fig. 5 illustrates the measured and full-wave simulated results. For BPF A^{DK}, the measured minimal insertion loss ($-20\log|S_{21}|$), 3-dB bandwidth, and center frequency are approximately 1.84 dB, 7.3%, and 2.4 GHz, respectively. For BPF B^{DK}, the measured minimal insertion loss ($-20\log|S_{31}|$), 3-dB bandwidth, and center frequency are approximately 1.88 dB, 6.9%, and 3.6GHz, respectively. Measured isolation ($-20\log|S_{32}|$) is >42 dB between two operating bands.

Fig. 6 demonstrates a layout and photograph of microstrip Diplexer B ($Z_{S/O}^{(D)} = 0\Omega$), wherein $R_2^{(D1)}$, $R_3^{(D1)}$, $R_2^{(D2)}$, and

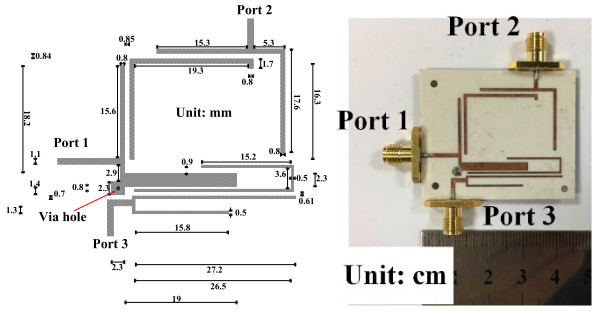

FIGURE 6. (a) Layout and (b) photograph of Diplexer B.

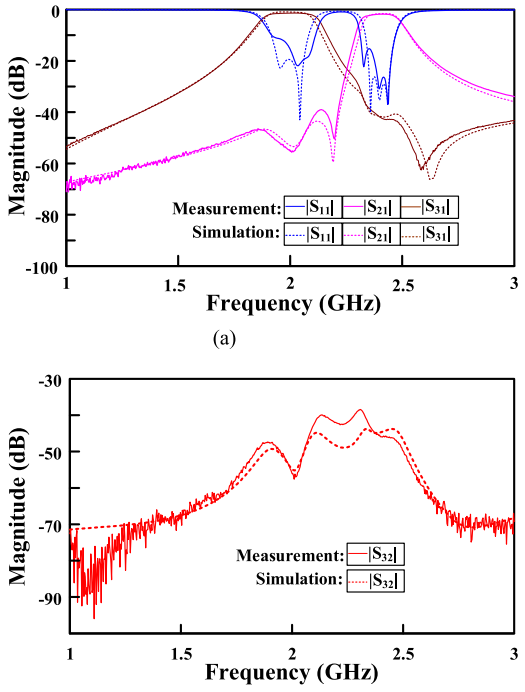

FIGURE 7. Measured and full-wave simulated results of Diplexer B. (a) $|S_{11}|$, $|S_{21}|$, and $|S_{31}|$, and (b) $|S_{32}|$.

$R_3^{(D2)}$ use $\lambda/2$ UIRs. Moreover, the via hole is used to implement $Z_{S/O}^{(D)} = 0\Omega$. Fig. 7 illustrates the measured and full-wave simulated results. For BPF A^{DK}, the measured minimal insertion loss ($-20\log|S_{21}|$), 3-dB bandwidth, and center frequency are approximately 1.84 dB, 7.6%, and 2.4 GHz, respectively. For BPF B^{DK}, the measured minimal insertion loss ($-20\log|S_{31}|$), 3-dB bandwidth, and center frequency are approximately 1.39 dB, 13.2%, and 1.995 GHz, respectively. Measured isolation ($-20\log|S_{32}|$) is >38 dB between two operating bands.

V. DISCUSSION OF CONVENTIONAL AND PROPOSED TRIPLEXERS

Fig. 8(a) displays a conventional triplexer using three tapped-line feed third-order filters [35]. Three matching lines $X_{M1}^{(T)}$,

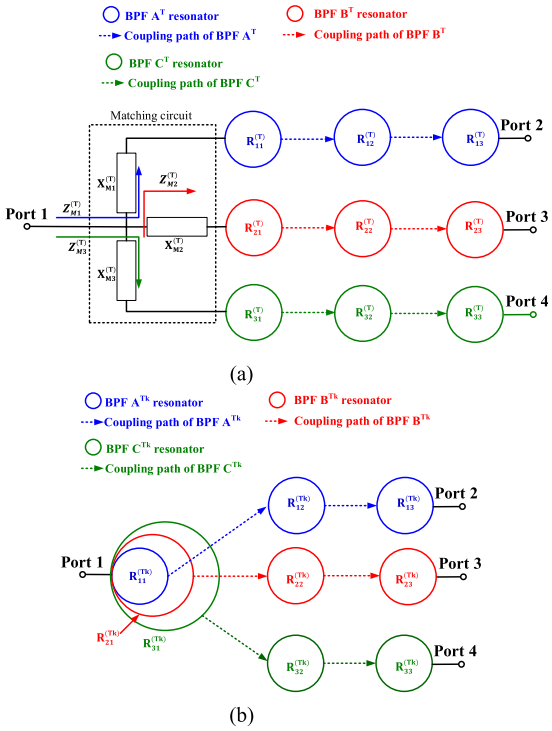

FIGURE 8. Using directed feed third-order filters for (a) conventional and (b) proposed triplexers.

$X_{M2}^{(T)}$, and $X_{M3}^{(T)}$ are added outside three different band third-order filters BPF A^T, BPF B^T, and BPF C^T to prevent the loading effect. However, the matching design of Fig. 8(a) typically needs a time-consuming optimum process because each channel circuit is required to meet one 50-Ω impedance matching and two open conditions. The proposed triplexer (Fig. 8(b)) includes three third-order filters BPF A^{TK}, BPF B^{TK} and BPF C^{TK}, whose center frequencies are f_1, f_2, and f_3, respectively. Resonator $R_{11}^{(Tk)}$ or $R_{21}^{(Tk)}$ is one part of resonator $R_{31}^{(Tk)}$ at the input port. In other words, resonator $R_{31}^{(Tk)}$ does not need additional circuit size to design resonator $R_{11}^{(Tk)}$ or resonator $R_{21}^{(Tk)}$. The Q_L of each band resonator can be designed independently by using integrated matching lines.

VI. DESIGN OF THE PROPOSED TRIPLEXER RESONATOR

To our knowledge, a systematic matching design for a triplexer without additional matching circuits outside the tapped-line feed filters [35] has not been reported thus far. The proposed stub-loaded resonator SLR T (Fig. 9) does not cost additional matching circuits outside the filters, and one of the three band input resonators can be shared by the other two-band input resonators, which demonstrates a high-integration design. The SLR T consisting of seven transmission lines $X_{T1}^{(T)}$, $X_{T2}^{(T)}$, $X_{T3}^{(T)}$, $X_{T4}^{(T)}$, $X_{T5}^{(T)}$, $X_{T6}^{(T)}$, and $X_{T7}^{(T)}$ with a load impedance $Z_{S/O}^{(T)}$ at one side end of $X_{T4}^{(D)}$ is shown in Fig. 9, wherein $Z_{S/O}^{(T)}$ can be designed as a short or open circuit causing SLR T to become similar to the stub-loaded resonator in [12] or net-type resonator in [34].

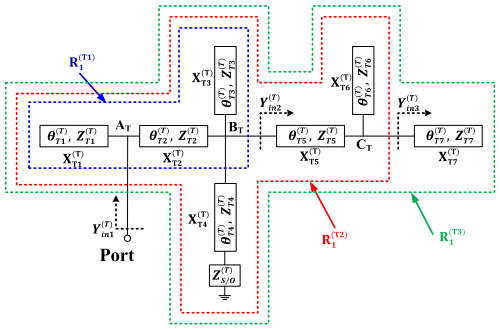

FIGURE 9. Proposed SLR T structure.

The SLR T is operated to resonate at three desired frequencies f_1, f_2, and f_3. $X_{T1}^{(T)}$, $X_{T2}^{(T)}$, and $X_{T3}^{(T)}$ are enclosed in the blue line form of the first resonator, $R_1^{(T1)}$, which resonates at f_1; $X_{T1}^{(T)}$, $X_{T2}^{(T)}$, $X_{T3}^{(T)}$, $X_{T4}^{(T)}$ with $Z_{S/O}^{(D)}$, $X_{T5}^{(T)}$, and $X_{T6}^{(T)}$ are enclosed in the red line form of the second resonator, $R_1^{(T2)}$, which resonates at f_2; and all of the transmission lines with $Z_{S/O}^{(D)}$ are enclosed in the green line form of the third resonator, $R_1^{(T3)}$, which resonates at f_3, wherein $\theta_{Ti}^{(T)}$ and $Z_{Ti}^{(T)} = 1/Y_{Ti}^{(T)}$, $i = 1-7$, represent electrical length and characteristic impedance, respectively.

Because the length of $X_{T3}^{(T)}$ is designed to be equal to $\lambda/4$ at f_1, Point B_T is a short circuit, causing $X_{T4}^{(T)}$ with $Z_{S/O}^{(D)}$, $X_{T5}^{(T)}$, $X_{T6}^{(T)}$, and $X_{T7}^{(T)}$ to have no loading effect for $R_1^{(T1)}$ at f_1. The total length of $X_{T1}^{(T)}$, $X_{T2}^{(T)}$, and $X_{T3}^{(T)}$ is $\lambda/2$ of f_1, and the characteristic impedance of $X_{T1}^{(T)}$ equals that of $X_{T2}^{(T)}$ (i.e., $R_1^{(T1)}$ composed of $X_{T1}^{(T)}$, $X_{T2}^{(T)}$, and $X_{T3}^{(T)}$ is a $\lambda/2$ resonator at f_1). The external quality factor of $R_1^{(T1)}$ can be designed by adjusting the length ratio of $\theta_{T1}^{(T)}$ and $\theta_{T2}^{(T)}$, such as tapped-line feed coupled-resonator filter [35].

The resonant condition of $R_1^{(T2)}$ at f_2 can be obtained by substituting the input admittance $Y_{in1}^{(T)}$ into (1). When the filter response specification at f_2 is determined, the required external quality factor of (2) is obtained. The length of $X_{T6}^{(T)}$ is designed to be equal to $\lambda/4$ at f_2. Point C_T is a short circuit, causing $X_{T7}^{(T)}$ to have no loading effect for $R_1^{(T2)}$ at f_2. Equations (1) and (2) include 12 design parameters of $R_1^{(T2)}$, which are $\theta_{Ti}^{(T)}$ and $Z_{Ti}^{(T)}$, $i = 1-6$. $\theta_{Ti}^{(T)}$ and $Z_{Ti}^{(T)}$, $i = 1-3$ are fixed and well-known when the design of resonator $R_1^{(T1)}$ at f_1 has been determined. Of the remaining five parameters $\theta_{T4}^{(T)}$, $\theta_{T5}^{(T)}$, $Z_{T4}^{(T)}$, $Z_{T5}^{(T)}$, and $Z_{T6}^{(T)}$, three can be arbitrarily designed, and the other two parameters can be solved using (1) and (2). The resonant condition of $R_1^{(T3)}$ at f_3 can be obtained by substituting the input admittance $Y_{in1}^{(T)}$ into (1). When the filter response specification at f_3 is determined, the required Q_L of (2) is obtained. Equations (1) and (2) include 14 design parameters of $R_1^{(T3)}$, which are $\theta_{Ti}^{(T)}$ and $Z_{Ti}^{(T)}$, $i = 1-7$. $\theta_{Ti}^{(D)}$ and $Z_{Ti}^{(T)}$, $i = 1-6$, are fixed and well-known when the design of resonator $R_1^{(T1)}$ at f_1 or $R_1^{(T2)}$ at f_2 is determined. The remaining two parameters $\theta_{T7}^{(T)}$ and $Z_{T7}^{(T)}$ can be solved by the equations (1) and (2). Furthermore, the resonant frequency and Q_L of $R_1^{(T1)}$ can also be designed by (1) and (2).

Based on the proposed SLR T design, each resonant frequency and Q_L of resonators $R_1^{(T1)}$, $R_1^{(T2)}$ and $R_1^{(D3)}$ can be systematically designed.

The SLR T with $Z_{S/O}^{(D)} = \infty\Omega$ and $Z_{S/O}^{(D)} = 0\Omega$ are used for designing the input resonator of Triplexer A and Triplexer B, respectively. The detailed equations of input admittance and external quality factor using (1) and (2) are shown as (6), shown at the bottom of this page, where

$$b_0 = \begin{cases} Y_{T4}^{(T)}\tan\theta_{T4}^{(T)}, & Z_{S/O}^{(T)} = \infty\Omega \\ -Y_{T4}^{(T)}\cot\theta_{T4}^{(T)}, & Z_{S/O}^{(T)} = 0\Omega \end{cases} \tag{7a}$$

and

$$b_1 = \frac{Y_{T5}^{(T)}\tan\theta_{T5}^{(T)}\cot\theta_{T6}^{(T)} + Y_{T6}^{(T)} + Y_{T7}^{(T)}\cot\theta_{T6}^{(T)}\tan\theta_{T7}^{(T)}}{Y_{T5}^{(T)}\tan\theta_{T5}^{(T)}\cot\theta_{T6}^{(T)} - Y_{T6}^{(T)} - Y_{T7}^{(T)}\cot\theta_{T6}^{(T)}\tan\theta_{T7}^{(T)}}. \tag{7b}$$

$$\begin{aligned} Q_L^{(T)} = {} & 25[c_0 - \frac{c_1c_2}{c_3} - \frac{c_1c_4}{c_3^2} \\ & \times \left(c_5 - c_6 + c_7 + c_8 - c_9 - \frac{c_{10}}{c_{11}} + \frac{c_{12}c_{13}}{c_{11}^2} - c_{14}\csc^2\theta_{T2}^{(T)}\right) \\ & + \frac{c_4}{c_3}(-c_5 - c_7 - c_8 + c_9 + \frac{c_{10}}{c_{11}} - \frac{c_{12}c_{13}}{c_{11}^2} \\ & + c_{14}\sec^2\theta_{T2}^{(T)} - c_{15})] \end{aligned} \tag{8}$$

where

$$c_0 = \theta_{T1}^{(T)}Y_{T1}^{(T)}\sec^2\theta_{T1}^{(T)} \tag{9a}$$

$$c_1 = Y_{T3}^{(T)} + b_0\cot\theta_{T3}^{(T)} + b_1Y_{T5}^{(T)}\cot\theta_{T3}^{(T)}\cot\theta_{T5}^{(T)} + Y_{T2}^{(T)}\cot\theta_{T3}^{(T)}\tan\theta_{T2}^{(T)} \tag{9b}$$

$$c_2 = \theta_{T2}^{(T)}Y_{T2}^{(T)}\csc^2\theta_{T2}^{(T)} \tag{9c}$$

$$c_3 = -Y_{T3}^{(T)} - b_0\cot\theta_{T3}^{(T)} - b_1Y_{T5}^{(T)}\cot\theta_{T3}^{(T)}\cot\theta_{T5}^{(T)} + Y_{T2}^{(T)}\cot\theta_{T2}^{(T)}\cot\theta_{T3}^{(T)} \tag{9d}$$

$$c_4 = Y_{T2}^{(T)}\cot\theta_{T2}^{(T)} \tag{9e}$$

$$c_5 = b_0\theta_{T3}^{(T)}\csc^2\theta_{T3}^{(T)} \tag{9f}$$

$$c_6 = \theta_{T3}^{(T)}Y_{T2}^{(T)}\cot\theta_{T2}^{(T)}\csc^2\theta_{T3}^{(T)} \tag{9g}$$

$$c_7 = b_1\theta_{T3}^{(T)}Y_{T5}^{(T)}\cot\theta_{T5}^{(T)}\csc^2\theta_{T3}^{(T)} \tag{9h}$$

$$c_8 = b_1\theta_{T5}^{(T)}Y_{T5}^{(T)}\cot\theta_{T3}^{(T)}\csc^2\theta_{T3}^{(T)} \tag{9i}$$

$$Y_{in1}^{(T)} = j\left(Y_{T1}^{(T)}\tan\theta_{T1}^{(T)} + Y_{T2}^{(T)}\cot\theta_{T2}^{(T)}\frac{Y_{T2}^{(T)}\tan\theta_{T2}^{(T)}\cot\theta_{T3}^{(T)} + Y_{T3}^{(T)} + b_0\cot\theta_{T3}^{(T)} + b_1Y_{T3}^{(T)}\cot\theta_{T3}^{(T)}\cot\theta_{T5}^{(T)}}{Y_{T2}^{(T)}\tan\theta_{T2}^{(T)}\cot\theta_{T3}^{(T)} - Y_{T3}^{(T)} - b_0\cot\theta_{T3}^{(T)} - b_1Y_{T3}^{(T)}\cot\theta_{T3}^{(T)}\cot\theta_{T5}^{(T)}}\right) = 0, \tag{6}$$

TABLE 3. Input circuit comparisons between proposed and previous triplexers.

	[3]	[8]	[16]	[20]	[21]	[24]	[28]	[29]	TA/TB
1**	y	n	y	y	n	n	y	y	n
2**	y	n	y	y	n	y	y	y	y
3**	n	n	n	n	y	y	n	n	n
4**	0	0	0	0	0	0	0	0	2
5**	n	y	n	n	n	n	n	n	y
6**	n	nm	y	y	nm	nm	n	n	y

1**: additional matching circuit outside the filters; 2**: independent Q_L designs for three band input resonators or independent designs for three band input circuits of filters facilitating design process; 3**: Q_L realization restricted by the distance between distributed-feed line and input resonator or long distributed-feed line length; 4**: number of integrated λ/4 matching lines in input resonator; 5**: three band input resonators integrated in one-band input resonator size for compact requirement; 6**: systematical input matching design for reducing time-consuming optimal process; TA: Triplexer A; TB: Triplexer B; y: yes; n: no; nm: no matching circuit.

$$c_9 = \begin{cases} \theta_{T4}^{(T)} Y_{T4}^{(T)} \cot\theta_{T3}^{(T)} \sec^2\theta_{T4}^{(T)} & \text{for } Z_{S/O}^{(T)} = \infty\Omega \\ \theta_{T4}^{(T)} Y_{T4}^{(T)} \cot\theta_{T3}^{(T)} \csc^2\theta_{T4}^{(T)} & \text{for } Z_{S/O}^{(T)} = 0\Omega \end{cases} \tag{9j}$$

$$\begin{aligned} c_{10} = {} & Y_{T5}^{(T)} \cot\theta_{T3}^{(T)} \cot\theta_{T5}^{(T)} (\theta_{T5}^{(T)} Y_{T5}^{(T)} \cot\theta_{T6}^{(T)} \sec^2\theta_{T5}^{(T)} \\ & + \theta_{T7}^{(T)} Y_{T7}^{(T)} \cot\theta_{T6}^{(T)} \sec^2\theta_{T7}^{(T)} - \theta_{T6}^{(T)} Y_{T5}^{(T)} \tan\theta_{T5}^{(T)} \csc^2\theta_{T6}^{(T)} \\ & - \theta_{T6}^{(T)} Y_{T7}^{(T)} \tan\theta_{T7}^{(T)} \csc^2\theta_{T6}^{(T)}) \end{aligned} \tag{9k}$$

$$c_{11} = -Y_{T6}^{(T)} + Y_{T5}^{(T)} \cot\theta_{T5}^{(T)} \cot\theta_{T6}^{(T)} - Y_{T7}^{(T)} \cot\theta_{T6}^{(T)} \tan\theta_{T7}^{(T)} \tag{9l}$$

$$\begin{aligned} c_{12} = {} & Y_{T5}^{(T)} \cot\theta_{T3}^{(T)} \cot\theta_{T5}^{(T)} (Y_{T6}^{(T)} + Y_{T5}^{(T)} \cot\theta_{T5}^{(T)} \cot\theta_{T6}^{(T)} \\ & + Y_{T7}^{(T)} \cot\theta_{T6}^{(T)} \tan\theta_{T7}^{(T)}) \end{aligned} \tag{9m}$$

$$\begin{aligned} c_{13} = {} & -\theta_{T5}^{(T)} Y_{T5}^{(T)} \cot\theta_{T6}^{(T)} \csc^2\theta_{T5}^{(T)} - \theta_{T6}^{(T)} Y_{T5}^{(T)} \cot\theta_{T5}^{(T)} \csc^2\theta_{T6}^{(T)} \\ & - \theta_{T7}^{(T)} Y_{T7}^{(T)} \cot\theta_{T6}^{(T)} \sec^2\theta_{T7}^{(T)} + \theta_{T6}^{(T)} Y_{T7}^{(T)} \csc^2\theta_{T6}^{(T)} \tan\theta_{T7}^{(T)} \end{aligned} \tag{9n}$$

$$c_{14} = \theta_{T2}^{(T)} Y_{T2}^{(T)} \cot\theta_{T3}^{(T)} \tag{9o}$$

$$c_{15} = \theta_{T3}^{(T)} Y_{T2}^{(T)} \tan\theta_{T2}^{(T)} \csc^2\theta_{T3}^{(T)}. \tag{9p}$$

Table 3 shows input circuit comparisons between proposed and previous triplexers.

VII. DESIGN OF THE PROPOSED TRIPLEXERS

Fig. 10 shows the proposed triplexer structure that has a third-order response in each transmission band and design procedure described as follows.

Step I$^{\mathrm{T}}$: The input resonator can follow the aforementioned SLR T in Section VI to design three-band resonance frequencies and external quality factors $Q_L^{(T1)}$ (for $\mathrm{R}_1^{(\mathrm{T1})}$), $Q_L^{(T2)}$ (for $\mathrm{R}_1^{(\mathrm{T2})}$), and $Q_L^{(T3)}$ (for $\mathrm{R}_1^{(\mathrm{T3})}$) based on the desired specification.

Step II$^{\mathrm{T}}$: Each band coupling coefficients are obtained using the tapped-line feed coupled-resonator filter design in [35]. In Fig. 10, $M_{ij}^{(Tk)}$ represents the coupling coefficient between resonators $\mathrm{R}_i^{(\mathrm{Tk})}$ and $\mathrm{R}_j^{(\mathrm{Tk})}$ at f_k, wherein $k = 1$, 2, or 3. The coupling $M_{12}^{(T1)}$ around f_2 or f_3 approaches zero because resonators $\mathrm{R}_1^{(\mathrm{T1})}$ and $\mathrm{R}_2^{(\mathrm{T1})}$ do not approach their resonant frequencies f_2 or f_3. In other words, the loading effect of $\mathrm{R}_1^{(\mathrm{T1})}$, from $\mathrm{R}_2^{(\mathrm{T1})}$ to Port 2 load, can be ignored around f_2 or f_3. The loading effect of $\mathrm{R}_1^{(\mathrm{T2})}$ or $\mathrm{R}_1^{(\mathrm{T3})}$ can similarly be ignored when it is not operated around its resonant frequency. Therefore, $\mathrm{R}_1^{(\mathrm{T1})}$, $\mathrm{R}_1^{(\mathrm{T2})}$, and $\mathrm{R}_1^{(\mathrm{T3})}$ can design their desired band coupling paths independently; a similar design concept has been validated in [6], [32], or [33].

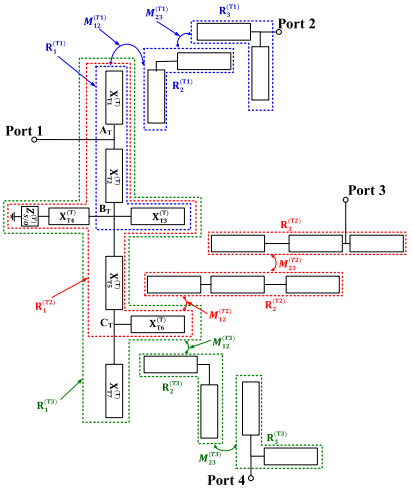

FIGURE 10. Proposed triplexer structure.

TABLE 4. Design Parameters of Triplexer A (TA) and Triplexer B (TB).

	$f_1/f_2/f_3$ (GHz)	$\theta_{T1}^{(T)}$ at f_1	$\theta_{T2}^{(T)}$ at f_1	$\theta_{T3}^{(T)}$ at f_1	$\theta_{T4}^{(T)}$ at f_1	$\theta_{T5}^{(T)}$ at f_1	$\theta_{T6}^{(T)}$ at f_2	$\theta_{T7}^{(T)}$ at f_1
	$Q_L^{(T1)}/Q_L^{(T2)}/Q_L^{(T3)}$	$Z_{T1}^{(T)}$ (Ω)	$Z_{T2}^{(T)}$ (Ω)	$Z_{T3}^{(T)}$ (Ω)	$Z_{T4}^{(T)}$ (Ω)	$Z_{T5}^{(T)}$ (Ω)	$Z_{T6}^{(T)}$ (Ω)	$Z_{T7}^{(T)}$ (Ω)
	$M_{12}^{(T1)}/M_{12}^{(T2)}/M_{12}^{(T3)}$							
	$M_{23}^{(T1)}/M_{23}^{(T2)}/M_{23}^{(T3)}$							
TA	2.4/1.9/3.7	77.3°	12.7°	90°	11.3°	15.04°	90°	20.19°
	16.12/15.1/18.08							
	0.063/0.067/0.056	80	80	47	41.5	46	48	57
	0.063/0.067/0.056							
TB	2.4/2/1.5	72.5°	17.5°	90°	8.22°	17.8°	90°	43.2°
	21.7/13.15/11.23							
	0.047/0.077/0.09	40	40	40	72.8	52	84.6	40
	0.047/0.077/0.09							

Step III$^{\mathrm{T}}$: Output external quality factors of $\mathrm{R}_3^{(\mathrm{T1})}$, $\mathrm{R}_3^{(\mathrm{T2})}$ and $\mathrm{R}_3^{(\mathrm{T3})}$ are equal to $Q_L^{(T1)}$, $Q_L^{(T2)}$, and $Q_L^{(T3)}$, respectively. The Q_{Ls} can be determined by feeding point, whose extraction method is in [35].

As a demonstration, three operating bands of microstrip Triplexer A ($Z_{S/O}^{(T)} = \infty\Omega$) and Triplexer B ($Z_{S/O}^{(D)} = 0\Omega$) are designed with 0.1 dB equal ripple filter responses. The related design parameters are illustrated in Table 4. Fig. 11 shows the layout and photograph of Triplexer A, wherein $\mathrm{R}_2^{(\mathrm{T1})}$, $\mathrm{R}_3^{(\mathrm{T1})}$, $\mathrm{R}_2^{(\mathrm{T3})}$, and $\mathrm{R}_3^{(\mathrm{T3})}$ use λ/2 UIRs; $\mathrm{R}_2^{(\mathrm{T2})}$ and $\mathrm{R}_3^{(\mathrm{T2})}$ of the stepped-impedance resonators design their spurious resonances not around $f_3 = 3.7$ GHz to prevent the loading effect affecting the BPF C$^{\mathrm{TK}}$ independent design. Fig. 12 shows the measured and full-wave simulated results. For BPF A$^{\mathrm{TK}}$, the measured minimal insertion loss ($-20\log|S_{21}|$), 3-dB bandwidth, and center frequency are approximately 2 dB, 7.4%, and 2.384 GHz, respectively. For BPF B$^{\mathrm{TK}}$, the measured minimal insertion loss ($-20\log|S_{31}|$), 3-dB bandwidth, and center frequency are approximately 1.438 dB, 11.9%, and 1.91GHz, respectively. For BPF C$^{\mathrm{TK}}$, the measured minimal insertion loss ($-20\log|S_{41}|$), 3-dB bandwidth, and center frequency are approximately 2.2 dB, 6.2%, and 3.67 GHz, respectively. Measured isolations $-20\log|S_{32}|$, $-20\log|S_{42}|$,

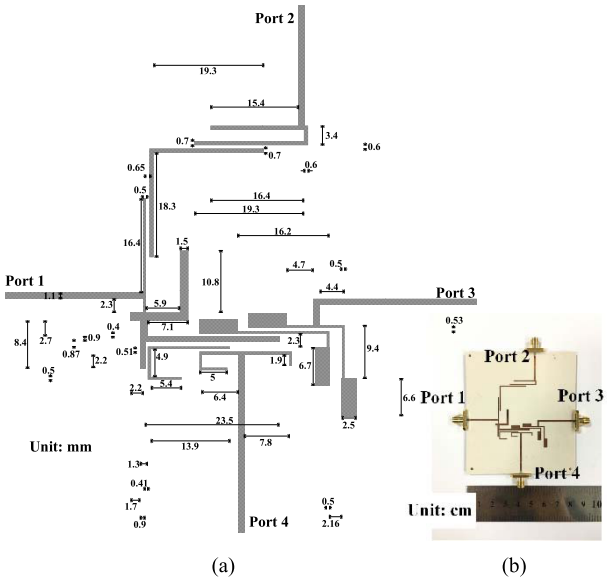

FIGURE 11. (a) Layout and (b) photograph of triplexer A.

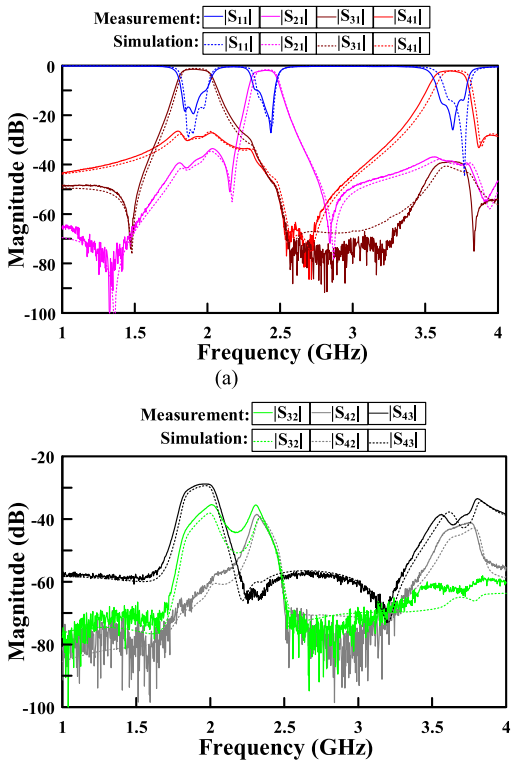

FIGURE 12. Measured and full-wave simulated results of triplexer A. (a) $|S_{11}|$, $|S_{21}|$, $|S_{31}|$, and $|S_{41}|$; and (b) $|S_{32}|$, $|S_{42}|$, and $|S_{43}|$.

and $-20\log|S_{43}|$ are >35, >38, and >28.8 dB, respectively, between the three operating bands.

Fig. 13 presents the layout and a photograph of microstrip Triplexer B, wherein the via hole is used to implement $Z_{S/O}^{(D)} = 0\Omega$; $R_2^{(T1)}$, $R_3^{(T1)}$, $R_2^{(T2)}$, $R_3^{(T3)}$, $R_2^{(T3)}$, and $R_3^{(T3)}$ use $\lambda/2$ UIRs. Fig. 14 shows the measured and full-wave

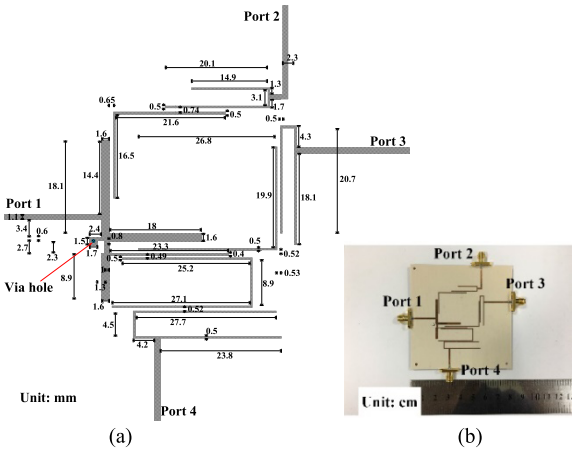

FIGURE 13. (a) Layout and (b) photograph of triplexer B.

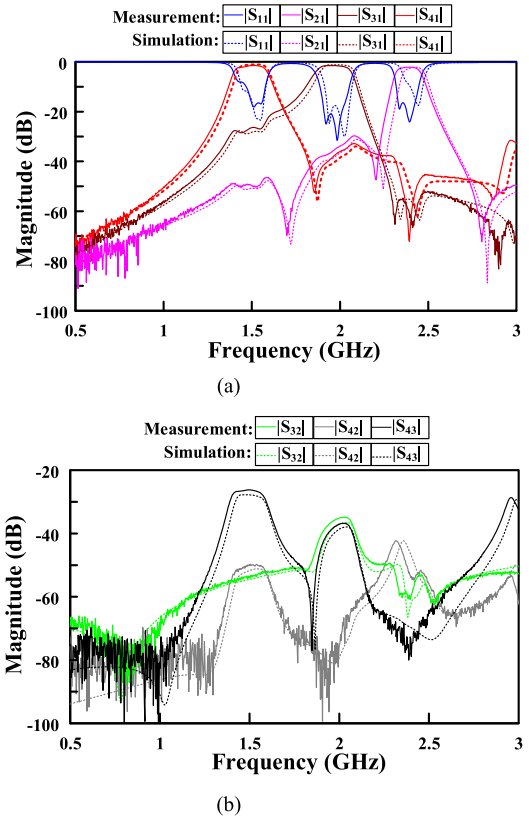

FIGURE 14. Measured and full-wave simulated results of triplexer B. (a) $|S_{11}|$, $|S_{21}|$, $|S_{31}|$, and $|S_{41}|$; and (b) $|S_{32}|$, $|S_{42}|$, and $|S_{43}|$.

simulated results. For BPF A^{TK}, the measured minimal insertion loss ($-20\log|S_{21}|$), 3-dB bandwidth, and center frequency are approximately 2.12 dB, 6.3%, and 2.393 GHz, respectively. For BPF B^{TK}, the measured minimal insertion loss ($-20\log|S_{31}|$), 3-dB bandwidth, and center frequency are approximately 1.5 dB, 10.8%, and 1.97 GHz, respectively. For BPF C^{TK}, the measured minimal insertion loss ($-20\log|S_{41}|$), 3-dB bandwidth, and center frequency are approximately 1.45 dB, 13%, and 1.5 GHz,

respectively. Measured isolations $-20\log|S_{32}|$, $-20\log|S_{42}|$, and $-20\log|S_{43}|$ are >34, >42, and >26 dB, respectively, between the three operating bands.

VIII. CONCLUSION

By using stub-loaded resonators with integration matching circuits, this study presents new diplexer and triplexer designs for effective and ease implementation on printed circuit boards. The proposed stub-loaded resonators (SLR D and SLR T) provide the required band matching conditions to avoid loading effects. SLR D and SLR T can systematically design all needed band Q_{Ls} and resonance frequencies. Furthermore, SLR D or SLR T only cost one-band resonator size and use the stub-loaded resonator to form the proposed diplexer and triplexer structures without additional matching circuits outside the filters. Therefore, each of the proposed circuits demonstrates high integration property. Besides, each isolation level of all presented circuits demonstrates serious noisy response about below than -50 dB which may be reasonable in general measured results under this low-level situation.

REFERENCES

[1] A. Sheta, J. Coupez, G. Tanne, S. Toutain, and J. Blot, "Miniature microstrip stepped impedance resonator bandpass filters and diplexers for mobile communications," in *IEEE MTT-S Int. Microw. Symp. Dig.*, Dec. 2002, pp. 607–610.
[2] C.-M. Tsai, S.-Y. Lee, C.-C. Chuang, and C.-C. Tsai, "A folded coupled-line structure and its application to filter and diplexer design," in *IEEE MTT-S Int. Microw. Symp. Dig.*, Jun. 2003, pp. 1927–1930.
[3] T. Ohno, K. Wada, and O. Hashimoto, "Design methodologies of planar duplexers and triplexers by manipulating attenuation poles," *IEEE Trans. Microw. Theory Techn.*, vol. 53, no. 6, pp. 2088–2095, Jun. 2005.
[4] S. Srisathit, S. Patisang, R. Phromloungsri, S. Bunnjaweht, S. Kosulvit, and M. Chongcheawchamnan, "High isolation and compact size microstrip hairpin diplexer," *IEEE Microw. Wireless Compon. Lett.*, vol. 15, no. 2, pp. 101–103, Feb. 2005.
[5] C.-W. Tang and S.-F. You, "Design methodologies of LTCC bandpass filters, diplexer, and triplexer with transmission zeros," *IEEE Trans. Microw. Theory Techn.*, vol. 54, no. 2, pp. 717–723, Feb. 2006.
[6] C.-F. Chen, T.-Y. Huang, C.-P. Chou, and R.-B. Wu, "Microstrip diplexers design with common resonator sections for compact size, but high isolation," *IEEE Trans. Microw. Theory Techn.*, vol. 54, no. 5, pp. 1945–1952, May 2006.
[7] T. Yang, P.-L. Chi, and T. Itoh, "High isolation and compact diplexer using the hybrid resonators," *IEEE Microw. Wireless Compon. Lett.*, vol. 20, no. 10, pp. 551–553, Oct. 2010.
[8] T. Yang, P.-L. Chi, and T. Itoh, "Compact quarter-wave resonator and its applications to miniaturized diplexer and triplexer," *IEEE Trans. Microw. Theory Techn.*, vol. 59, no. 2, pp. 260–269, Feb. 2011.
[9] M.-L. Chuang and M.-T. Wu, "Microstrip diplexer design using common T-shaped resonator," *IEEE Microw. Wireless Compon. Lett.*, vol. 21, no. 11, pp. 583–585, Nov. 2011.
[10] J.-Y. Zou, C.-H. Wu, and T.-G. Ma, "Miniaturized diplexer using synthesized microstrip lines with series LC tanks," *IEEE Microw. Wireless Compon. Lett.*, vol. 22, no. 7, pp. 354–356, Jul. 2012.
[11] H. Liu, W. Xu, Z. Zhang, and X. Guan, "Compact diplexer using slotline stepped impedance resonator," *IEEE Microw. Wireless Compon. Lett.*, vol. 23, no. 2, pp. 75–77, Feb. 2013.
[12] C.-F. Chen, C.-Y. Lin, B.-H. Tseng, and S.-F. Chang, "High-isolation and high-rejection microstrip diplexer with independently controllable transmission zeros," *IEEE Microw. Wireless Compon. Lett.*, vol. 24, no. 12, pp. 851–853, Dec. 2014.
[13] Q. Shao, F.-C. Chen, and Q.-X. Chu, "Design of compact six-channel diplexer using crossed resonators," in *Proc. 6th Asia–Pacific Conf. Antennas Propag. (APCAP)*, Oct. 2017, pp. 1–3.
[14] X. Guan, W. Liu, B. Ren, H. Liu, and P. Wen, "A novel design method for high isolated microstrip diplexers without extra matching circuit," *IEEE Access*, vol. 7, pp. 119681–119688, 2019.
[15] P.-H. Deng and J.-T. Tsai, "Design of microstrip lowpass-bandpass diplexer," *IEEE Microw. Wireless Compon. Lett.*, vol. 23, no. 7, pp. 332–334, Jul. 2013.
[16] P.-H. Deng, M.-I. Lai, S.-K. Jeng, and C. H. Chen, "Design of matching circuits for microstrip triplexers based on stepped-impedance resonators," *IEEE Trans. Microw. Theory Techn.*, vol. 54, no. 12, pp. 4185–4192, Dec. 2006.
[17] S. Cadiou, C. Quendo, E. Rius, J. F. Favennec, B. Potelon, R. Segalen, and F. Mahé, "An 11–18 GHz four-channel DBR multiplexer for electronic warfare systems," in *Proc. Eur. Microw. Conf.*, Sep. 2009, pp. 679–682.
[18] S.-J. Zeng, J.-Y. Wu, and W.-H. Tu, "Compact and high-isolation quadruplexer using distributed coupling technique," *IEEE Microw. Wireless Compon. Lett.*, vol. 21, no. 4, pp. 197–199, Apr. 2011.
[19] C.-F. Chen, T.-M. Shen, T.-Y. Huang, and R.-B. Wu, "Design of compact quadruplexer based on the tri-mode net-type resonators," *IEEE Microw. Wireless Compon. Lett.*, vol. 21, no. 10, pp. 534–536, Oct. 2011.
[20] H. Lee and T. Itoh, "Dual band isolation circuits based on CRLH transmission lines for triplexer application," in *Proc. Asia–Pacific Microw. Conf.*, Dec. 2011, pp. 542–545.
[21] J.-Y. Wu, K.-W. Hsu, Y.-H. Tseng, and W.-H. Tu, "High-isolation microstrip triplexer using multiple-mode resonators," *IEEE Microw. Wireless Compon. Lett.*, vol. 22, no. 4, pp. 173–175, Apr. 2012.
[22] H. Lee and T. Itoh, "Tri-band isolation circuits based on double-Lorentz transmission lines for quadruplexers," in *Proc. 42nd Eur. Microw. Conf.*, Oct. 2012, pp. 585–588.
[23] S. Taravati and M. Khalaj-Amirhosseini, "Design method for matching circuits of general multiplexers," *IET Microw., Antennas Propag.*, vol. 7, no. 4, pp. 237–244, Mar. 2013.
[24] H.-W. Wu, S.-H. Huang, and Y.-F. Chen, "Compact microstrip triplexer based on coupled stepped impedance resonators," in *IEEE MTT-S Int. Microw. Symp. Dig.*, Jun. 2013, pp. 1–3.
[25] H. Lee and T. Itoh, "Tri-band isolation circuits using both stop-band and pass-band of double-Lorentz transmission lines for quadruplexers," in *IEEE MTT-S Int. Microw. Symp. Dig. (MTT)*, Jun. 2013, pp. 1–3.
[26] C.-H. Lai, W.-S. Chung, and T.-G. Ma, "On-chip miniaturized triplexer using lumped networks with dual resonators on an integrated passive device process," *IEEE Trans. Microw. Theory Techn.*, vol. 62, no. 12, pp. 2923–2930, Dec. 2014.
[27] P.-H. Deng, B.-L. Huang, and B.-L. Chen, "Designs of microstrip four- and five-channel multiplexers using branch-line-shaped matching circuits," *IEEE Trans. Compon., Packag., Manuf. Technol.*, vol. 5, no. 9, pp. 1331–1338, Sep. 2015.
[28] S.-C. Lin and C.-Y. Yeh, "Design of microstrip triplexer with high isolation based on parallel coupled-line filters using T-shaped short-circuited resonators," *IEEE Microw. Wireless Compon. Lett.*, vol. 25, no. 10, pp. 648–650, Oct. 2015.
[29] K. D. Xu, M. Li, Y. Liu, Y. Yang, and Q. H. Liu, "Design of triplexer using E-stub-loaded composite right-/left-handed resonators and quasi-lumped impedance matching network," *IEEE Access*, vol. 6, pp. 18814–18821, 2018.
[30] Y. Chu, K. Ma, and Y. Wang, "A novel triplexer based on SISL platform," *IEEE Trans. Microw. Theory Techn.*, vol. 67, no. 3, pp. 997–1004, Mar. 2019.
[31] C.-H. Lai, C.-Y. Shiau, and T.-G. Ma, "Microwave three-channel selector using tri-mode synthesized transmission lines," *IEEE Trans. Microw. Theory Techn.*, vol. 61, no. 10, pp. 3529–3540, Oct. 2013.
[32] P.-H. Deng and H.-H. Tung, "Design of microstrip dual-passband filter based on branch-line resonators," *IEEE Microw. Wireless Compon. Lett.*, vol. 21, no. 4, pp. 200–202, Apr. 2011.
[33] P. H. Deng, P. T. Chiu, C. P. Yang, and L. C. Dai, "Design of dual-band filters utilizing new branch-line resonators," in *Proc. Asia–Pacific Microw. Conf.*, Dec. 2011, pp. 912–915.
[34] C. F. Chen, T. Y. Huang, and R. B. Wu, "A miniaturized net-type microstrip bandpass filter using $\lambda/8$ resonators," *IEEE Microw. Wireless Compon. Lett.*, vol. 15, no. 7, pp. 481–483, Jul. 2005.
[35] J. Wong, "Microstrip tapped-line filter design," *IEEE Trans. Microw. Theory Techn.*, vol. MTT-27, no. 1, pp. 44–50, Jan. 1979.
[36] J.-T. Kuo and E. Shih, "Microstrip stepped impedance resonator bandpass filter with an extended optimal rejection bandwidth," *IEEE Trans. Microw. Theory Techn.*, vol. 51, no. 5, pp. 1554–1559, May 2003.

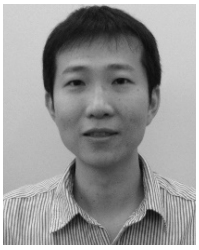

PU-HUA DENG (Member, IEEE) was born in Kaohsiung, Taiwan, in 1978. He received the B.Sc. degree in electrical engineering from National Sun Yat-sen University, Kaohsiung, Taiwan, in 2002, and the M.Sc. and Ph.D. degrees in communication engineering from National Taiwan University, Taipei, Taiwan, in 2004 and 2006, respectively.

In 2006, he joined ZyXEL Communications Corporation, Hsinchu, Taiwan, where he was a RF Engineer. In 2007, he joined NXP Semiconductors Company, Kaohsiung, Taiwan, where he was an Advanced RF Testing Engineer. From August 2008 to January 2009, he joined the Faculty of the Department of Electrical Engineering, National University of Tainan, Tainan, Taiwan, as an Assistant Professor. Since 2009, he joined the Faculty of the Department of Electrical Engineering, National University of Kaohsiung, Kaohsiung, Taiwan, where he is currently a Professor. His research interest includes the design and analysis of microwave planar circuits.

SHENG-WEI LEI was born in Kaohsiung, Taiwan, in 1972. He received the B.S. degree in electrical engineering from I-Shou University, Kaohsiung, Taiwan, in 1997, and the M.S. degree from the Institute of Communications Engineering, National Chiao Tung University, Hsinchu, Taiwan, in 1999. Since 2019, he has been with MediaTek Inc., Hsinchu, Taiwan, where he is currently a Technical Manager of Testing Engineering Division on RF and Millimeter Wave Testing Circuit Development.

WEI LO was born in Kaohsiung, Taiwan, in 1991. He received the M.S. degree in electrical engineering from the National University of Kaohsiung, Kaohsiung, Taiwan, in 2016. He is currently with the Super Micro Computer, CA, USA.

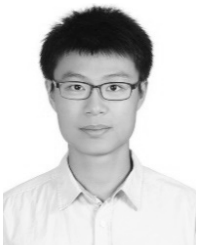

MING-WEI LI was born in Taipei, Taiwan, in 1995. He received the B.S. degree in electrical engineering from the National University of Kaohsiung, Kaohsiung, Taiwan, in 2018. He is currently pursuing the M.S. degree with the National Tsing Hua University, Hsinchu, Taiwan.

He is currently with the Institute of Photonics Technologies, National Tsing Hua University, where he is involved in optical communication.